Image Anal Stereol 2001;20(Suppl 1):504-509

USE OF IMAGE ANALYSIS AND FINITE ELEMENT ANALYSIS TO CHARACTERISE FLUID FLOW IN ROUGH ROCK FRACTURES AND THEIR SYTHETIC ANALOGUES

STEVEN OGILVIE, EVGENY ISAKOV, COLIN TAYLOR AND PAUL GLOVER

Department of Geology and Petroleum Geology, University of Aberdeen, Aberdeen AB24 3UE, Scotland
e-mail: s.ogilvie@abdn.ac.uk, e.isakov@abdn.ac.uk, c.w.taylor@abdn.ac.uk, p.glover@abdn.ac.uk

ABSTRACT

Fracture surface roughness has significant control on the movement of fluids through fractures in the Earth's crust. To quantify this influence we have image-analysed experimentally determined fluid flow in a range of rock fractures and compared these observations with numerical modelling of fluid flow through the fractures. The image analysis was performed on resin replicas of rock fracture surfaces with emphasis placed upon the variation of flow rate with fracture fabric. These high fidelity polymer models were also profiled in a highly controlled manner using in-house developed hardware and image analysis software (OptiProf™). Statistical analysis of the surfaces provides the necessary input for the creation of numerical models, the boundary conditions of which are used in flow modelling. This integrated approach enables the physical constraints on fluid flow in rough fractures to be well characterised.

Keywords: fluid flow, image analysis, modelling, polymer models, rock fractures.

INTRODUCTION

Integrated studies of the geometry of fracture networks and flow processes in single fractures are necessary to understand the bulk contribution of fractures to fluid flow. Surface roughness plays a major role in the conductivity of fluids through fractures leading to increased tortuosity, turbulence and dispersion (due to channelling) in fluid/dissolved contaminant transport (Brown, 1987; Glover *et al*., 1997; 1998a; 1998b). The majority of work concerns theoretical studies of fluid flow through rough fractures with only a small body of recent research involving *in-situ* descriptions of the flow paths (e.g., Brown *et al*., 1998; Dijk *et al*., 1999; Durham *et al*., 2001).

We have carried out (i) image analysis of experimentally determined fluid flow, and (ii) numerical modelling of fluid flow in natural rock fractures. The experimental work involved the imaging of fluid flow through resin replicas of fractures surfaces, termed high fidelity polymer models (HFPMs). The HFPMs are arranged to allow "fabric-parallel" flow and "cross-fabric" flow in the anisotropic rocks studied. Fluid flow was modelled in 2D and 3D in the measured rock fractures and suites of synthetic fractures. The fluid flow modelling was carried out in a FEMLAB™ environment. Numerical modelling was carried out by solving the partial differential equations in synthetic fractures created from the original fractures using image analysed parameters and a finite element approach.

The HFPM models were also used to provide high resolution profiling measurements of each rough fracture surface (resolution: 15×15×15 μm) using in-house developed hardware and image analysis software (OptiProf™) that incorporates image improvement and noise suppression features (Ogilvie *et al*., this volume). The resulting profiled fracture surfaces can be married to provide numerical fracture surface topography and aperture maps that can be used directly in numerical fluid flow modelling. Alternatively, the measured surface topography and aperture map can be analysed, by further software developed in-house (ParaFrac™), to derive the characteristic statistical and fractal properties that describe the fracture. Suites of synthetic fractures are generated from this data using in-house developed SynFrac™ software. Synthetic fractures are quick and easy to create, and once the initial parameters are known any number of different fractures with the same properties may be created. The synthesis procedure is fully described in Isakov *et al*. (this volume).

METHODS AND MEASUREMENT

SAMPLE PREPARATION

Transparent high fidelity polymer models (HFPMs) of a suite of natural fracture surfaces were created (*xy*-size 100×100 mm). These have a very high fidelity of reproduction (*xyz*-resolution < 1 μm) as illustrated in Ogilvie *et al.*, (this volume). Here, they are used for imaging during flow experiments, however, each fracture half has been used in the pointwise determination of fracture aperture by calibrating the Lambert-Beer Law (Ogilvie *et al*., this volume). The HFPMs are carefully mated and loaded into a cell (Fig. 1). Two HFPM cells were prepared for a sample of syenite to allow (i) flow along the fabric of the rock and (ii) flow against the fabric of the rock while tracking fluid flow through them by using a digital optical imaging (DOI) technique. The cells have input and output flow ports to receive the fluids at controlled rates and pressures, and have fluid flow manifolds to distribute the fluid evenly across the fracture surface.

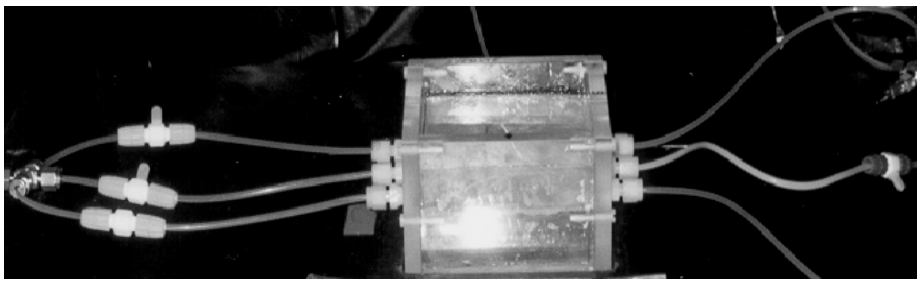

Fig. 1. *An HFPM of syenite in position under the digital camera and above the light (box) source. Fluid inflow pipes (and peristaltic pump) are to the right and outflow is to the left.*

DIGITAL OPTICAL IMAGING SET-UP

The DOI apparatus consists of a high quality digital colour camera mounted on a frame, directed towards a light box. The camera gives a lateral resolution of 15-200 μm for imaged areas of 10×10 mm and 100×100 mm respectively, and a vertical resolution of about 15 μm for 8-bit grey-scale depth. The light box was covered with a black rubber mat around the HFPM and surrounded by black-out curtains to shield the imaging process from ambient and reflected light. Light can be transmitted directly across the fracture plane allowing fluid flow processes to be observed with a video camera under a variety of conditions (e.g., fluid flow-rate, density, viscosity, fluid phases, pressure-difference, immiscibility). A transparent area of approximately 100×100 mm in the fracture plane was available for viewing.

EXPERIMENTAL FLUID FLOW

The HFPMs were kept horizontal on the light box to minimise effects of gravity flow and were cleaned by flushing water, containing flakes of detergent through them. They were then dried using compressed air. Brown *et al*. (1998) found that the resin casts used in their study were slightly hydrophilic, especially when surfaces had been wet before or the air was humid. The surfaces were therefore wetted using water. After wetting, water was flushed through each HFPM at a flow rate (charge) of 9 ml/min using a peristaltic pump (to achieve a steady-state of flow) into three input pipes (Fig. 1). The Reynolds Number is an important parameter describing flow through fracture apertures, which represents the relative importance of inertial versus viscous forces. A Reynolds Number, $Re = \rho Q/\mu L = 1.5$ is calculated for the above flow charge, Q, water density, ρ, viscosity, μ and HFPM width, L. The water is then replaced with a higher concentration of dyed water (5 g/1), than that used for aperture determinations. This is primarily for visualisation purposes. The images can then be analysed to provide local flow velocities, vorticity, and channelling.

The images were captured and stored at approximately 1 minute intervals for both flow orientations in timeframes using Adobe Premier 5.1™ software. Fluid pressure was held constant along two opposite sides of the fracture, and a pressure gradient was set up across the fracture by setting the pressure on each ide to different values. This can be read from manometers on the tubing at

either side of the apparatus. A back-pressure is applied to fill regions of low aperture by turning a valve at the outflow end of the apparatus.

FLOW MODELLING

Fluid flow was modelled in 2D and 3D in the measured rock fractures and suites of synthetic fractures. The fluid flow modelling was carried out in a FEMLAB™ environment. The image analysed surface topography and aperture maps were used to define the physical boundaries of the model. A fine triangular finite element grid was set-up in the fracture using iteratively refined Delaunay triangulation. The fluid input face was defined to have a constant flow boundary condition with a parabolic profile, and the fluid output face was set to zero pressure. The rough surfaces of the fracture has non-slip boundary conditions and the remaining sides of the fracture, were given symmetrical (slip) boundary conditions. The two linked partial differential equations that were solved were (i) incompressible Navier-Stokes equation and (ii) the mass balance equation. Modelling was carried out as a function of flow rate, scale, density and viscosity, resulting in Reynolds numbers, $0.01 \leq Re \leq 20$.

EXPERIMENTAL FLUID FLOW

The following results are concerned with flow through HFPMs of a sample of syenite. The anisotropy in this sample is shown by coarse laths of plagioclase, which define an East-West fabric (A in Fig. 2). This rock has a core-plug (helium) porosity of 0.20% and a Hassler-Sleeve (nitrogen) gas permeability of 0.02 mD. It is therefore likely that the majority of flow in such a rock would be accommodated by fracture systems.

There are clear differences in fluid behaviour when fluid is pumped along the fabric of the HFPM (Fig. 2) compared to "across fabric" flow (Fig. 3). This is in accordance with the work of Patir and Cheng (1978) who show that when the roughness has a strong directional fabric, flow rate can be different from flow rate for isotropic roughness. In fact, Thompson and Brown (1991) state that directional anisotropy has greater influence upon fluid and electrical transport in fractures than surface roughness.

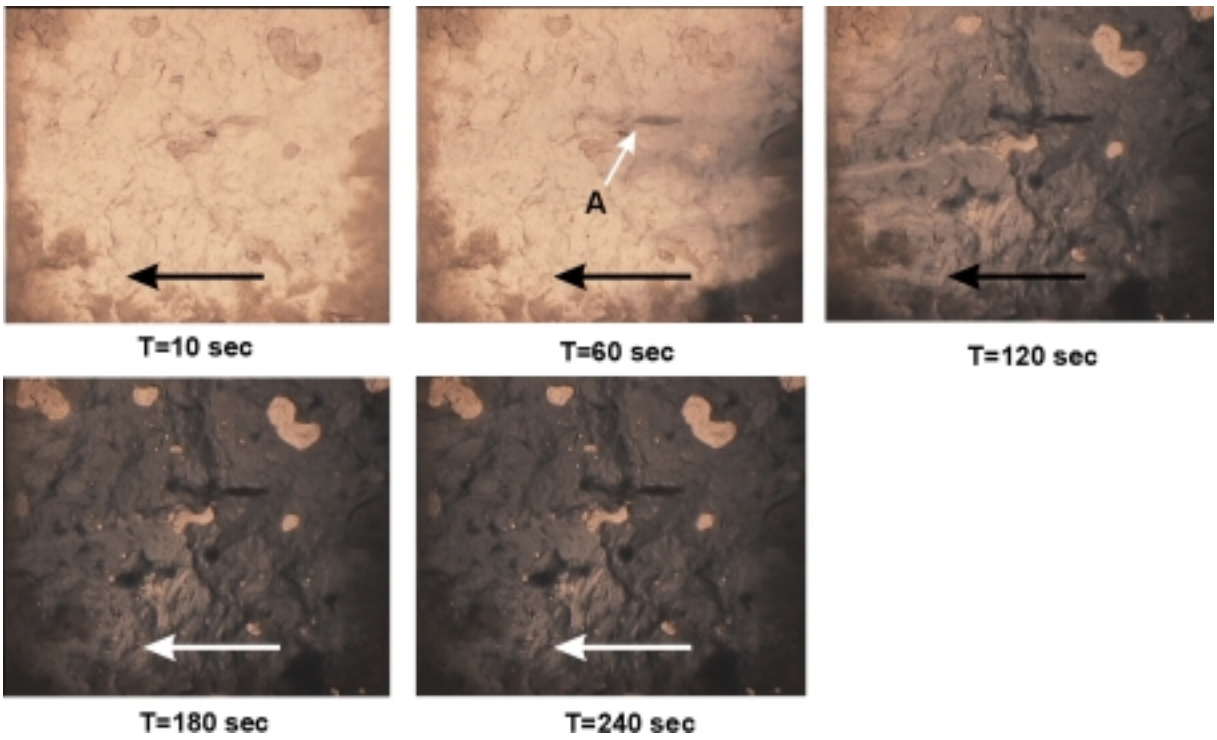

Fig. 2. *Frames showing the transport of dyed water (replacing undyed water) into an HFPM cell of syenite sample with flow along the fabric of the model (from right to left). Flow rate is 9 ml/min and Reynolds Number calculated as 1.5. Distinct channelling of the flow is observed by the evolution of streamlines on the 2 minutes time frame. The HFPM is completely filled in 5 minutes.*

With “fabric-parallel” flow (Fig. 2) the streamlines appear more regular and the flow is generally more organised than that against the fabric (Fig. 3). Furthermore, the HFPM with flow against the fabric (Fig. 3) takes longer to fill as evidenced by comparison of the equivalent time frames in Fig. 2. For example, a combination of low aperture and textural barriers discourage the fluid from transgressing centrally through the HFPM. Streamlines can, however, be seen curving into the central area within 2 minutes. These are accentuated by the presence of water bubbles which drain water into the streamlines. Significant ponding of fluid can be seen behind a wall of N-S running plagioclase crystals (A in Fig. 3), which show up a continuous dark area from 2 minutes to near saturation at 4 minutes.

Local turbulence or instability of flow is not observed in either situation; the flow is laminar even along the walls of the HFPM.

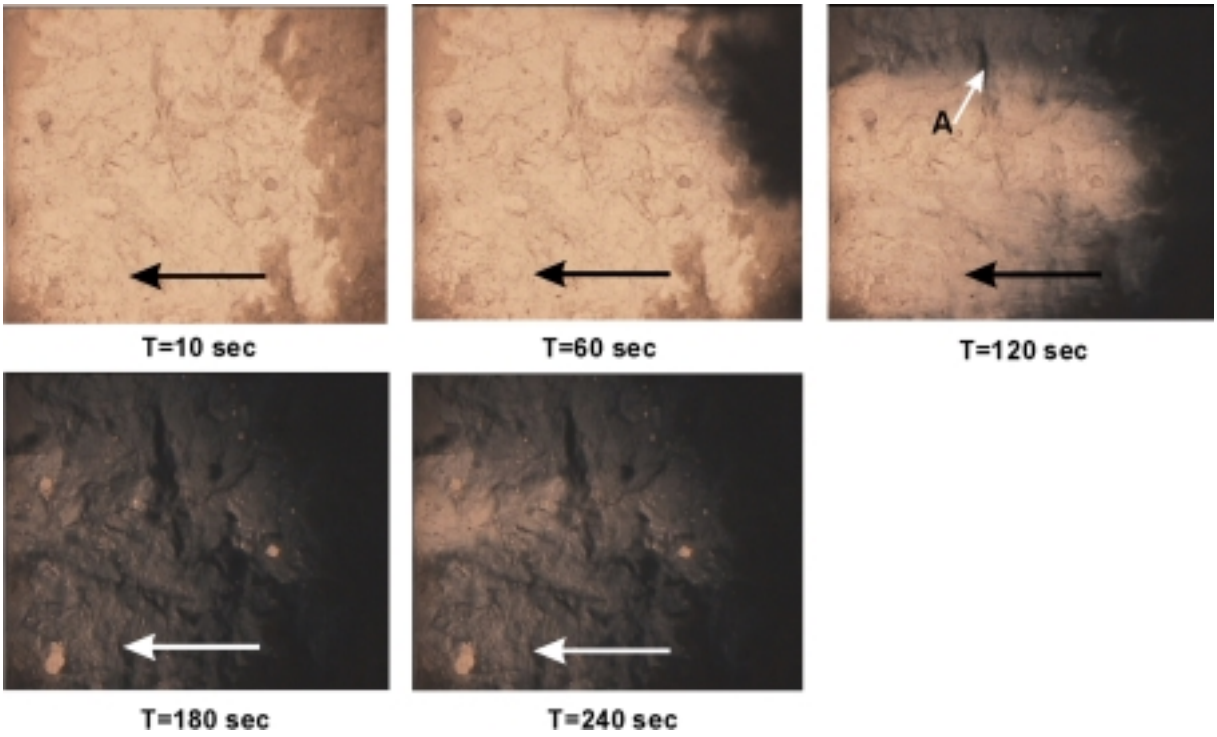

Fig. 3. *Transport of dyed water (replacing undyed water) into HFPM cell of syenite sample with fluid flow ports positioned at 90° to HFPM in Fig. 2 i.e., flow is against the fabric. Flow is from right to left (arrow). The cell fills more gradually than the HFPM in Fig 2.*

MODELLED FLUID FLOW

Modelling in both 2D and 3D has shown large variations in the nature of the fluid transport processes as a function of (i) flow rate, (ii) the fluid density, (iii) the fluid viscosity, (iv) the size of the fracture, and hence (v) Reynolds number, and also (vi) the scale of the fracture relative to the geometric mean aperture (2D case) and dual mean aperture (3D case). The dual mean has been implemented to avoid zero mean aperture values where fracture surfaces touch at a single point. It is the geometric mean aperture for each profile in the direction of gross flow, arithmetically averaged across all such profiles.

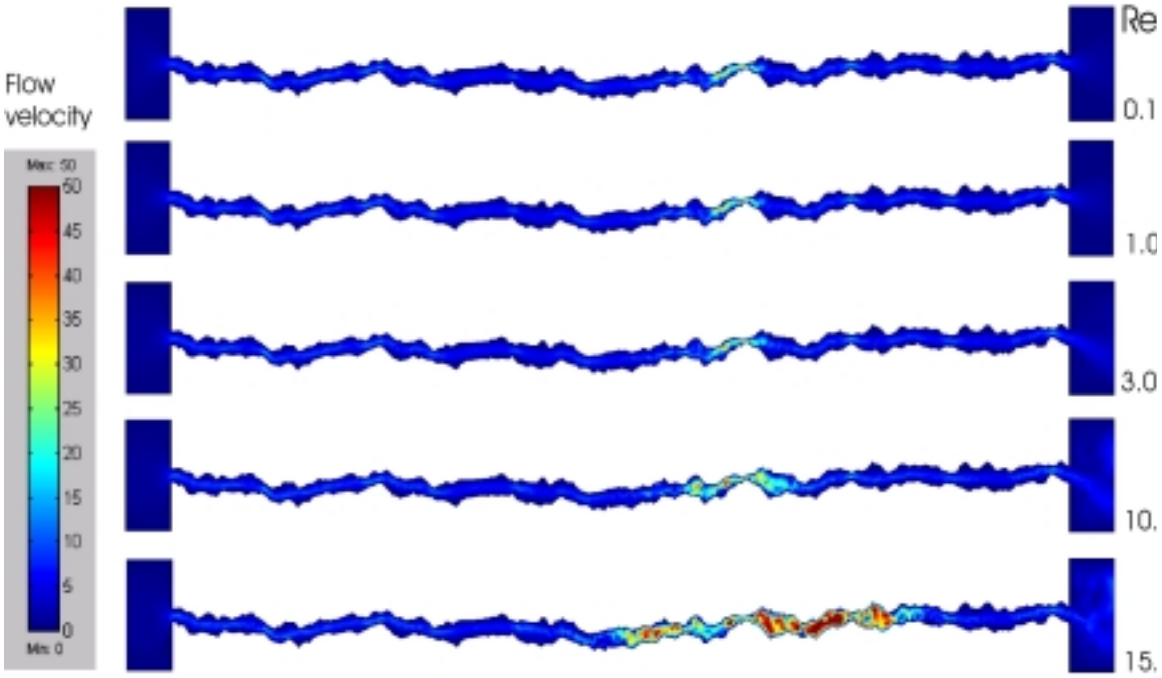

Fig. 4. *Numerical solution of a series of flows through a synthetic fracture tuned to the fracture imaged in Figs. 2 and 3. Re = Reynolds number; Scale shows flow rate (Vo).*

A series of simulations of flow through 2D fracture cross-sections are illustrated in Fig. 4. The fracture profiles were measured and synthesised with SynFrac^{TM} (Isakov *et al*., this volume). Flow is from left to right. The flow scale to the left of the diagram is divided into V_o units i.e., the maximum velocity of the parabolic profile at the input end. The Reynolds Numbers were counted at the input end of the simulations. At low Reynolds numbers (Re = 0.1 – 1) the flow state approximates that of the viscous flow limit and inertial forces are non-existent. Therefore, the flow pattern is qualitatively the same. As the Reynolds Number increases, inertial forces play a greater role in the fluid flow e.g., at Re = 3, one can observe jet-type behaviour at the outflow end of the simulation. Further increases in the Reynolds Number causes the appearance of flow disturbances within the bottle-neck in the central part of the fracture. These spread in both the upstream and downstream directions. As the Reynolds Number reaches *c.* 15, the flow becomes unstable.

DISCUSSION AND CONCLUSIONS

Boundary conditions from flow experiments of resin replicas (HFPMs) of rough fracture surfaces and from synthetic models of these fractures (Isakov *et al*., this volume) are used as input into 2D flow models.

Initial results from this study show that the combination of the modelling and experimental image analysis approach has potential for enabling the physical constraints on fluid flow in rough fractures to be well characterised.

ACKNOLWEDGMENT

This work is sponsored by NERC as part of the Micro-Macro thematic programme ongoing in the UK.

REFERENCES

Brown SR (1987). Fluid Flow through rock joints: The effect of surface roughness. J Geophys Res 92:1337-47.

Brown S, Caprihan A, Hardy R (1998). Experimental observation of fluid flow channels in a single fracture. J Geophys Res 103:5125-32.

Dijk P, Berkowitz B, Bendel P (1999). Investigation of flow in water-saturated rock fractures using nuclear

magnetic resonance imaging (NMRI). Water Resour Res 35:347-60.

Durham WB, Bourcier WL, Burton EA (2001). Direct observation of reactive flow in a single fracture. Water Resour Res 37:1-12.

Glover PWJ, Matsuki K, Hikima R, Hayashi K (1997). Fluid flow in fractally rough synthetic fractures. Geophys Res Lett 24:1803-6.

Glover PWJ, Matsuki K, Hikima R, Hayashi K (1998a). Synthetic rough fractures in rocks. J Geophys Res 103:9609-20.

Glover PWJ, Matsuki K, Hikima R, Hayashi K (1998b). Fluid flow in synthetic rough fractures and application to the Hachimantai geothermal HDR test site. J Geophys Res 103(B5):9621-35.

Patir N, Cheng HS (1978). An average flow model for determining effects of three-dimensional roughness on partial hydrodynamic lubrication. J Lubric Technol 100:12-7.

Thompson ME, Brown SR (1991). The effect of anisotropic surface roughness on flow and transport in fractures. J Geophys Res 96(B13):21923-32.